ORGANIC CHEMISTRY FRONTIERS

RESEARCH ARTICLE

View Article Online
View Journal

Cite this: DOI: 10.1039/d5qo00708a

An efficient method for the synthesis of π-expanded phosphonium salts†

Krzysztof Górski, [a] Łukasz W. Ciszewski, [a] Antoni Wrzosek, [b] Adam Szewczyk, *[b] Andrzej L. Sobolewski *[c] and Daniel T. Gryko *[a]

A new straightforward methodology for the synthesis of phosphonium salts integrated with a π-conjugated scaffold has been developed using phosphine oxides. It is now possible to obtain cyclic phosphonium salts possessing up to eight conjugated rings and bearing *e.g.* pyrrole, thiophene, indole or benzofuran scaffolds from abundant and commercially available materials in high yields. An enticing feature of this general strategy is that this one-step procedure typically does not require chromatographic purification. Still greater synthetic possibilities are related to the fact that even demanding scaffolds such as azulene, pyrene or fluorene can be bridged with the phospholium subunit. Starting from 1,4-dihydropyrrolo[3,2-*b*]pyrrole, heretofore rarely observed ladder-type bis-phosphonium salts were effectively prepared. This strategy was also extended into the preparation of cyclic arsonium salt. The ability to form phosphonium salts possessing such manifold scaffolds translated into diverse photophysical properties ranging from non-fluorescent dyes to thiophene-derivatives emitting quantitatively in the blue region. Geometry change induced by light absorption has a predominant influence on the fate of the molecules' excited state. It was shown, in analogy to previous results, that cyclic tetraarylphosphonium salts migrate through the membrane of living cells to localize in the mitochondria similarly to the well-known triarylphosphonium salts.

Received 30th April 2025,
Accepted 1st June 2025

DOI: 10.1039/d5qo00708a

rsc.li/frontiers-organic

Introduction

Heterocyclic analogs of polycyclic aromatic hydrocarbons possessing phosphorus atom(s) have received considerably less systematic attention than architectures possessing oxygen, nitrogen and sulfur.[1,2] Extensive efforts have been devoted to advancing such classes as phosphines,[3,4] phosphine oxides,[5,6] phosholes[7–12] and phosphonium salts.[13–35] In the most recent years, new possibilities were discovered also for phosphorines,[36–38] azaphospholes[39,40] and phosphaquinolin-2-ones.[41,42] As far as electronegativity, valence and coordination number are concerned, phosphorus is quite specific compared to other heteroatoms. For these reasons, studies of the impact of its insertion on the optical/redox properties of PAHs are intense and have led to the discovery of materials with promising optoelectronic properties.[3] Among various architectures, phosphonium salts possessing one or two σ^4,λ^4-P^+ are relatively less explored.[13–34] Most employed routes towards phosphonium salts is S_N2 quaternization of σ^3,λ^3-P cyclic chromophores. This, however, requires pre-synthesized cyclic phosphines.[17–19,21,23,28,30–34] Several annulation methods of *ortho*-alkynyl arylphosphines have directly led to the formation of benzo[*b*]phospholium salts, in gold[43] or acid-catalyzed processes[25] (Scheme 1A). π-Expanded phosphonium salts have also been prepared through Cu-catalyzed C–H functionalization[13,24] or electrolysis[44] of appropriately substituted arylphosphines (Scheme 1B). In 2010 Manabe and Ishikawa described the cyclization of [1,1′-biphenyl]-2-yldicyclohexylphosphane in the presence of Tf_2O (Scheme 1C).[45] Later on, Miura *et al.* reported that diarylphosphine oxides undergo Tf_2O-catalyzed cyclization to form phosphine oxides (Scheme 1D).[46] An analogous idea has also been reported for reaction with alkynes.[47,48] Inspired by these reports, we decided to develop a straightforward synthetic protocol for the conversion of triarylphosphine oxides into cyclic phosphonium salts, which would be one of the most concise routes toward these valuable compounds (Scheme 1E).

[a]*Institute of Organic Chemistry Polish Academy of Sciences, Kasprzaka 44-52, 01-224 Warsaw, Poland. E-mail: daniel.gryko@icho.edu.pl*
[b]*Nencki Institute of Experimental Biology Polish Academy of Sciences, Pasteura, Warsaw, Poland. E-mail: a.szewczyk@nencki.gov.pl*
[c]*Institute of Physics Polish Academy of Sciences, Al. Lotników 32/46, 02-667 Warsaw, Poland. E-mail: sobola@ifpan.edu.pl*

†Electronic supplementary information (ESI) available: Synthetic procedures, NMR spectra, UV-Vis spectra, cyclic voltammograms, and characteristics, computational details, Cartesian coordinates of ground and excited states, and X-ray structure details. CCDC 2405937 (**2i**). For ESI and crystallographic data in CIF or other electronic format see DOI: **https://doi.org/10.1039/d5qo00708a**

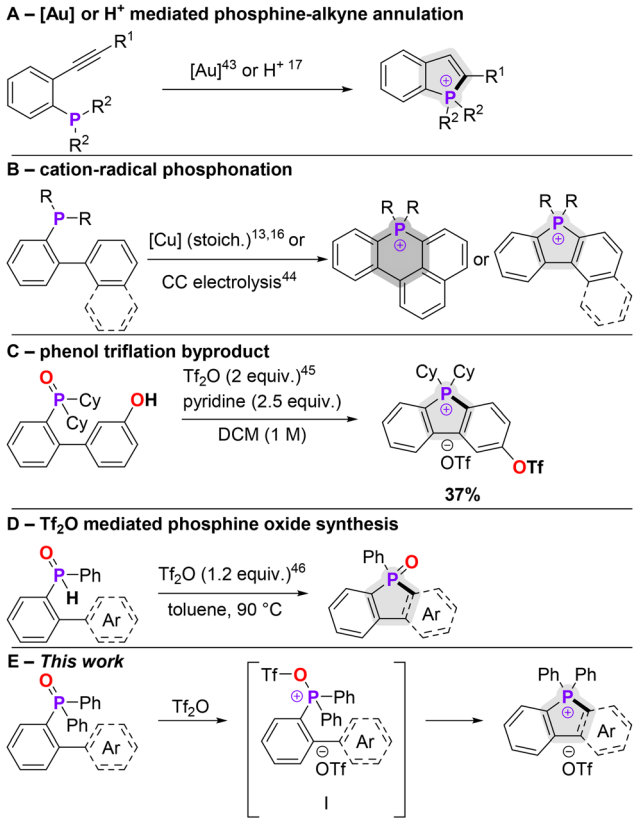

Scheme 1 Selected synthetic methods for cyclic diarylphosphonium salts.

Results and discussion

Synthesis

To our delight, the reaction of phosphine oxide **1a** with trifluoromethanesulfonic anhydride in the presence of diisopropylethylamine (DIPEA) yielded the formation of phospholium salt **2a** in a quantitative yield after just 1 hour (Scheme 2). A quick evaluation revealed that a similar result is observed when the reaction is conducted without the addition of a base. Furthermore, under these conditions, the purification of the products was greatly simplified. We thus synthesized a series of phosphine oxides (**1b–x**), to evaluate the method's scope and limitations and subsequently subjected these compounds to the optimized reaction conditions (Scheme 2). Intramolecular electrophilic attack on 5-membered heteroaromatic rings of thiophene, benzothiophene, benzofuran and indoles resulted in the formation of new five-membered phospholium rings in good yields and without the need for chromatographic purification of the products **2a–f,h–i,p,t–v,x** and **4a–b**. Most salts can be easily isolated from the reaction mixture by suspending them in 10% methanol or isopropanol in diethyl ether, followed by filtration.

Based on earlier precedence and especially on Miura's papers,[46–48] a plausible reaction mechanism was proposed (Scheme S1†). Initially, after the attack of triflic anhydride on phosphorus atom, the intermediate phosphonium salt forms. Subsequently the attack of this salt as an electrophile on aromatic ring leads to the formation of P–C bond and formation of five-membered ring (phosphacyclic intermediate). Finally, an elimination of triflic acid affords the final product.

Surprisingly, furan derivative **1c** required an alternative set of conditions, which included employing toluene as the solvent and increasing the temperature to achieve a full conversion of the substrate and yield 68% of dye **2c**. For phosphine oxide **1f**, containing an indolic N–H bond, only C3 substitution product **2f** was observed. Moreover, for indole derivatives **2h** and **2i** successful formation of corresponding 6- and 7-membered rings was observed, showcasing the broad versatility of the method. The latter product's structure was confirmed with the aid of X-ray crystallography (CCDC 2405937, Fig. S251†). The positive outcome of the transformation observed on electron-rich aromatic rings encouraged us to try the method for π-expansion of more sophisticated systems – namely 1,4-dihydropyrrolo[3,2-*b*]pyrroles (DHPP).[49,50] Specially designed substrates **1j–n** were synthesized and subjected to the optimized reaction conditions. DHPPs are known to be unstable under acidic conditions.[49,50] In order to prevent acid-induced decomposition of both products and substrates, the transformation was conducted in the presence of DIPEA. The same base was used for other substrates possessing very electron-rich scaffolds which are prone to acid-induced decomposition *i.e.* **2h** and **2q**. Centrosymmetric dyes **2j–l** bearing a DHPP scaffold were formed in good yields, despite lowered nucleophilicity of the aromatic system after the first electrophilic attack (Scheme 2).

Unsymmetrical derivative **2m** was formed in a slightly diminished yield and a similar outcome was observed for the consecutive formation of two 6-membered rings in compound **2n**. Moreover, the C–P bond formation at the benzene ring decorated with electron-donating substituents was tested. Despite bearing only one electron-donating group, 5-oxatruxene derivative **2o** was formed under the milder set of conditions, however, in diminished yields (Scheme 2).

Though efficient transformation of other monosubstituted phosphine oxides **1r,s** required more vigorous conditions, corresponding products were formed in very good yields. On the other hand, 1,3-dimethoxydibenzo[*b*,*d*]phospholium **2t** was efficiently formed at room temperature. The discovered methodology's usefulness toward the modification of electron-rich systems prompted us to test it for the synthesis of PAHs-derived phosphonium salts. Guaiazulene derivative **2u** was obtained under the milder set of conditions in a decent yield. On the other hand, phosphonium indeno[2,1-*a*]pyrene, dibenzo[*f*,*ij*]tetraphene and benzo[*a*]aceanthrylene analogues **2v–x** were efficiently formed upon treating phosphine oxides **1v–x** with Tf_2O in toluene at 90 °C (Scheme 2).

Intrigued by the broad scope of the developed strategy, we inspected whether the described reaction could also be utilized in an intermolecular process. Subjecting electron-rich arene to the phosphine oxide resulted in the formation of tetraarylphosphonium salt in good yields (with 46% for **4a**,

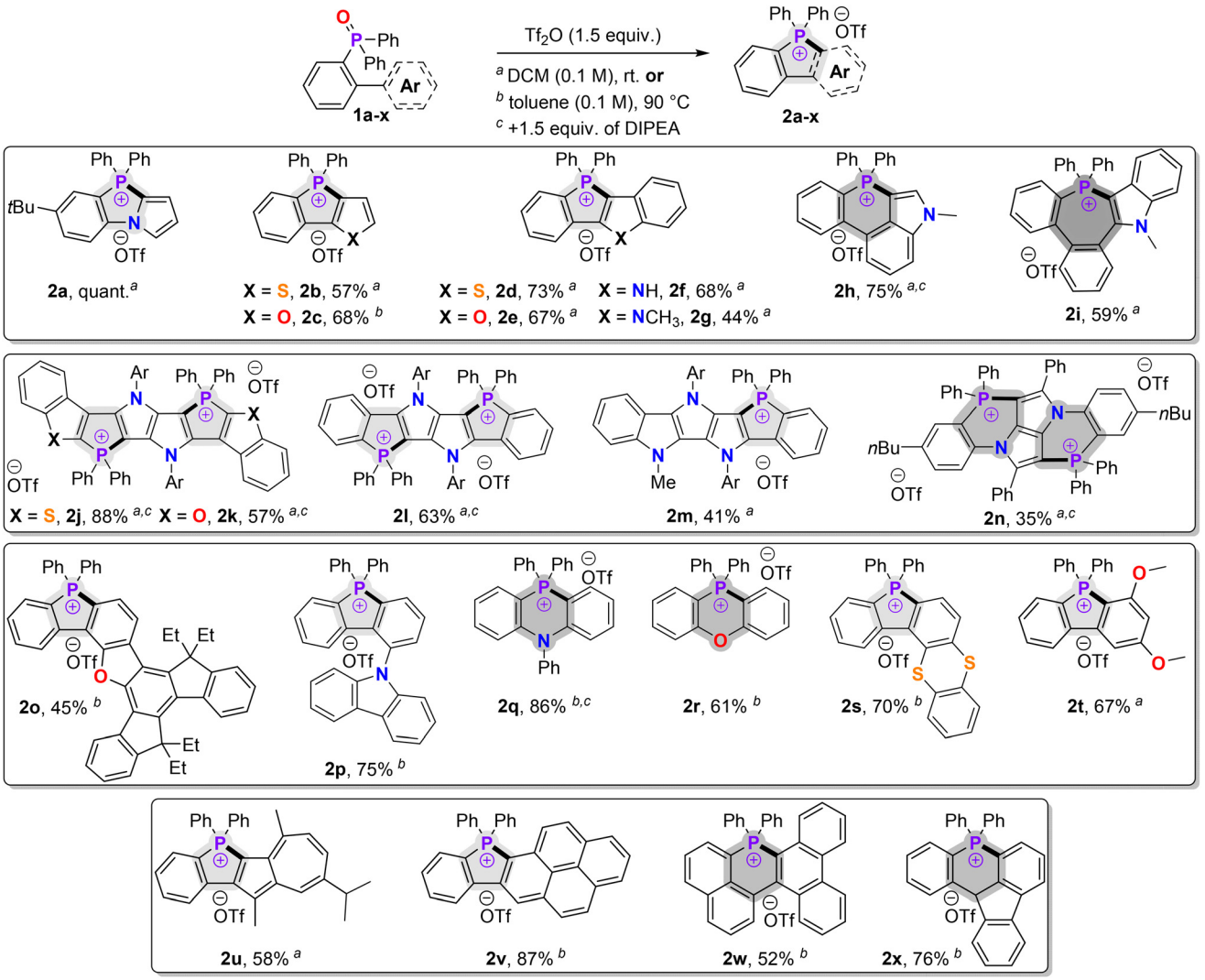

Scheme 2 Scope and limitations of the transformation of phosphine oxides into phosphonium salts. Ar = 4-*n*Bu-C_6H_4- isolated yields, conditions: [a] DCM, rt, [b] toluene 90 °C, [c] reaction was conducted in the presence of 1.5 equiv. of DIPEA.

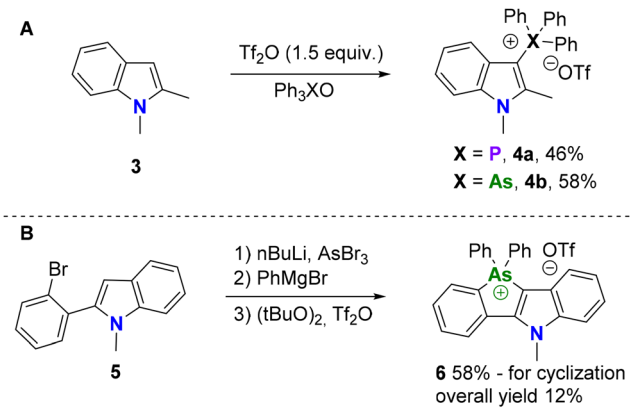

Scheme 3 A – Intermolecular variant of the transformation, B – one-pot synthesis of arsolium salt.

Scheme 3A). Encouraged by this result, we attempted to widen the scope to include arsenic derivatives (as it is an element from the same periodic table row). Experiments revealed that arsine oxides also undergo this reaction, leading to, among others, the corresponding tetraarylarsonium derivative **4b** (58%). The results prompted us to examine an intramolecular variant of arsine oxide cyclization. We thus discovered that the presence of an indole subunit increases the instability of the obtained arsine, however, fast workup enables its isolation. Further oxidation furnishes arsine oxide, which turned out to be unstable and decomposed to a yellow substance. Hence, alternative conditions were developed allowing one-step oxidation and cyclization. Utilization of di-*t*-butylperoxide, which is commonly used as a radical initiator,[51] in the presence of Tf_2O, turned out to be an inert oxygen source, allowing arsolium ring incorporation with a 58% reaction yield for **6** (Scheme 3B).

Electrochemistry

The electrochemical properties of the synthesized compounds were studied using cyclic voltammetry. For most of them, irreversible reduction events were detected, with the onset potential values ranging between −1.40 V (*vs.* Fc/Fc$^+$ couple) for guaiazulene derivative **2u** and −2.32 V for acyclic salt **4a**. Replacing MeCN with DMF and 1,2-dichloroethane has not altered the irreversibility of reduction (Fig. S226 and S227†). However, for PAH analogues **2v** and **2w**, a reversible reduction process could be observed (Table S1, Fig. S219–S243†). Despite being cationic, the products could also be electrochemically oxidized, as observed on the cyclic voltammograms in the form of irreversible events at onset potentials ranging from 0.95 V (*vs.* Fc/Fc$^+$ couple) for **2u** to 1.61 V for dimethoxybenzene derived product **2t**. An even lower-lying reversible oxidation event was observed at $E^{ox}_{1/2}$ = 0.33 V *vs.* Fc/Fc$^+$ for the unsymmetrical DHPP derivative **2m**. Measured onset oxidation and reduction potentials were utilized to evaluate the HOMO and LUMO energies of the phosphonium salts (*vide infra*).

Experimental and computational analysis of photophysical properties

Photophysical properties of phosphonium salts were measured in dichloromethane, tetrahydrofuran, acetonitrile and solid state (Table 1, Table S1, Fig. S162–S210†). Similarly to other organic dyes, the optical properties can be modulated by π-electron system expansion,[52] heteroatom exchange[53] or introduction of electron-donating or electron-withdrawing substituents.[54,55] Thus, absorption spectra cover a wide range of the UV-Vis spectrum, starting from λ_{abs} = 288 nm for **4a** up

Table 1 Spectroscopic data in dichloromethane (red), tetrahydrofuran (orange), and acetonitrile (blue) for phosphonium salts

Salt	λ_{abs} [nm] ($\varepsilon \times 10^{-3}$ [cm^{-1} M^{-1}])	λ_{em} [nm]	$\Delta\nu$ [cm^{-1}]	Φ_{FL} [%]	Salt	λ_{abs} [nm] ($\varepsilon \times 10^{-3}$ [cm^{-1} M^{-1}])	λ_{em} [nm]	$\Delta\nu$ [cm^{-1}]	Φ_{FL} [%]
2a	341 (1.9)	426	5900	10	**2n**	361 (3.2)	463	6100	62
	338 (1.6)	428	6200	15		358 (3.7)	465	6400	62
	336 (1.6)	429	6500	17		356 (3.1)	468	6700	52
2b	350 (3.9)	433	5500	≈100	**2o**	352 (8.1), 407 (1.9)	530	5700	17
	349 (3.3)	445	6200	≈100		347 (6.9), 402 (1.4)	530	6000	15
	348 (3.3)	440	6000	≈100		343 (9.2), 391 (2.2)	550	7400	11
2c	346 (2.9)	440	6200	72	**2p**	333 (7.8), 387 (0.9)	535	7100	11
	343 (2.6)	459	7400	75		333 (8.2), 375 (1.0)	567	9000	5.4
	344 (2.9)	448	6700	86		333 (8.2), 371 (0.9)	559	9100	4.3
2d	340 (3.9), 368 (3.0)	460	5400	61	**2q**	344 (10.6), 355 (10.0)	388	2400	5.4
	338 (3.4), 366 (2.5)	464	5800	62		344 (10.5), 355 (9.9)	388	2400	5.2
	334 (3.6), 364 (2.8)	462	5800	61		344 (10.3), 355 (9.6)	390	2500	4.7
2e	360 (5.4)	460	6000	69	**2r**	300 (8.9), 307 (8.5)	328	2100	3.4
	353 (5.7)	467	6900	69		301 (6.9), 307 (7.1)	329	2200	6.1
	353 (5.0)	466	6900	68		300 (7.2), 306 (7.4)	329	2300	3.0
2f	304 (12.8), 371 (3.7)	490	6500	57	**2s**	371 (3.5)	557	9000	8.0
	301 (17.8), 354 (4.4)	493	8000	59		366 (2.9)	575	9900	11
	301 (19.8), 356 (4.9)	491	7700	63		366 (3.4)	583	10 200	9.1
2f[a]	315 (19.3)	577	n.d.	2.2	**2t**	329 (7.5), 336 (7.4)	387	3900	7.9
	319 (12.9)	577	n.d.	2.2		328 (7.8), 337 (7.4)	390	4000	4.5
	313 (26.7)	577	n.d.	2.1		328 (7.5), 335 (7.2)	390	4200	3.6
2g	371 (3.8)	490	6500	89	**2u**	394 (13.4), 562 (1.3)	n.d.	n.d.	n.d
	370 (3.2)	500	7000	≈100		394 (14.7), 561 (1.3)	418, 441. 698	3500	<0.001
	364 (3.7)	500	7500	93		392 (13.7), 559 (1.4)	n.d.	n.d.	n.d.
2h	350 (13.2), 363 (11.3)	401	2600	30	**2v**	401 (12.7), 425 (15.7)	434, 456	500	91
	352 (12.7), 364 (11.1)	410	3100	89		400 (10.5), 424 (13.6)	434, 458	500	97
	348 (13.0), 360 (11.4)	410	3400	83		398 (10.3), 422 (13.5)	434, 455	700	93
2i	278 (19.2), 300 (15.8)	399	8300	2.4	**2w**	388 (12.1)	466	4300	9.9
	277 (18.7), 301 (15.5)	414	9100	2.6		387 (11.8)	466	4400	8.6
	276 (18.3), 298 (15.3)	426	10 100	2.3		387 (11.3)	466	4400	10
2j	506 (13.5)	633	4000	19	**2x**	378 (0.3), 590 (0.1)	351	n.d.	13
	504 (12.3)	640	4200	27		379 (3.1), 602 (1.2)	n.d.	n.d.	n.d.
	489 (3.7)	640	4800	19		370 (4.2), 582 (2.0)	355, 652	n.d.	5.5*
2k	483 (6.3)	642	5100	0.8	**2x′**[a]	465 (5.7), 590 (5.7)	657	1700	0.5
	485 (6.9)	633	4800	0.4					
	463 (3.0)	659	6400	<0.001					
2l	322 (28.7), 427 (15.3)	523	4300	60	**4a**	274 (12.9), 287 (10.0)	n.d.	n.d.	n.d.
	324 (35.3), 429 (17.4)	542	4900	75		275 (17.0), 287 (13.7)	n.d.	n.d.	n.d.
	321 (25.9), 422 (13.8)	539	5100	51		274 (32.4)	n.d.	n.d.	n.d.
2m	362 (31.3), 460 (7.0)	672	6900	2.0	**4b**	279 (10.8), 288 (9.5)	n.d.	n.d.	n.d.
	358 (30.3), 450 (6.7)	672	7300	1.1		280 (13.7), 288 (12.1)	n.d.	n.d.	n.d.
	355 (31.8), 442 (7.1)	705	8400	0.4		279 (10.8), 287 (9.7)	n.d.	n.d.	n.d.
					6	361 (5.2)	472, 486	6500	<0.001
						362 (5.2)	440	4900	0.1
						358 (5.1)	n.d.	n.d.	n.d.

$\lambda_{abs}/\lambda_{em}$ – absorption/emission wavelength, ε – molar absorption coefficient, $\Delta\nu$ – Stokes shift, Φ_{FL} – fluorescence quantum yield, # – determined for transition between S_0 and S_1 states, * – determined for two emission bands, [a] – measured after addition of 100 μl of DBU.

to 602 nm for **2x** and are affected by solvent polarity, changing molar extinction coefficient (ε), shape and absorption maxima (λ_{abs}) for most studied dyes.[56] According to Table 1, most salts containing 5-membered phospholium subunit (**2a–e,g,o,s**), possess $\varepsilon \leq 5000$ M^{-1} cm^{-1} for the most red-shifted bands, which stand in line with rather low oscillator strengths (Tables S3, S5, S7, S9, S11 and S15†) for the $S_0 \rightarrow S_1$ electron transitions (f = 0.1–0.2). The $S_0 \rightarrow S_1$ transition for the simple phospholium salts is described by the HOMO–LUMO configuration. As presented in *e.g.* Table S3,† the Highest Occupied Molecular Orbital (HOMO) electron density is located at molecule's periphery, while Lowest Molecular Unoccupied Orbital (LUMO) it is mostly concentrated within the distinctly acceptor phosphacycle. Therefore, photon absorption initiates an electron density shift from the molecule's periphery toward the P^+ center. On the other hand, ring expansion to a 6-membered phosphorinium doesn't change the first excitation orbital configuration. However, electron density distribution over LUMO becomes less affected by the P^+ center, while at HOMO it is mostly maintained, which results in rising oscillator strength, f = 0.313 (Tables S16 and S17†), and ε up to 11 000 M^{-1} cm^{-1} for **2h** (Table 1).

Positively charged phosphacycles share another feature, namely, large Stokes shifts ($\Delta\nu$), starting from ≈2000 cm^{-1} for **2q,r** up to 10 000 cm^{-1} for **2i,s** (Table 1). Moreover, comparing emission spectra *vs.* solvent polarity reveals a solvatofluorochromic response, which becomes more pronounced as the π-electron system expands, like for **2m** (Fig. 1). Nevertheless, a lack of strict correlation with solvent polarity (Table S2, Fig. S209 and S210†) suggests that the solvatochromic response must be related to complex solvation processes.

In typical donor–acceptor compounds, an immense $\Delta\nu$ and solvatofluorochromism are related to excitation-driven changes in electric dipole moment,[57,58] which is not the case in the discussed charged phosphacycles. More in-depth analysis performed on model systems **2b**, **2g**, **2k** and **2m** in a broader range of solvents and utilizing E_T (30) parameter,[59] as well as a more detailed solvation model[60] didn't provide an appropriate correlation (Table S2, Fig. S209–S218†). However indicates that the solvatofluorochromism primarily depends on two solvent parameters: basicity and dipolarity. Thus, the origin of the observed phenomena must be related to differences in cation solvation in both the ground (^{1}GS) and excited states (^{1}LE), as well as the geometrical changes arising upon excitation (Fig. 2).

Photon absorption-driven changes in molecular geometry also significantly impact the fate of the molecule in the excited state. A computational study of a few selected molecules (see ESI†) reveals that, disregarding the triplet states population, the photophysics of cations is primarily a competition between the local excited state (^{1}LE) and the so-called charge transfer state (^{1}CT). The electron density at ^{1}CT indicates that electron transfer occurs from the π-system to the P^+ or As^+ centres, leading to distinct geometrical changes. The consequence of formal charge separation is vanishingly small oscillator strength for the $^1CT \rightarrow {}^1GS$ electronic transition, which, combined with a remarkable decrease in the ^{1}CT state energy, makes the deactivation of the excited state through ^{1}CT the main nonradiative channel.

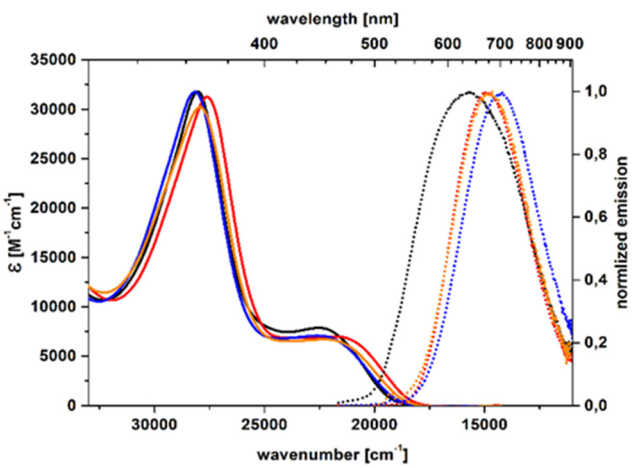

Fig. 1 Absorption (solid) and emission (dot) spectra of **2m** in toluene (black), dichloromethane (red), tetrahydrofuran (orange) and acetonitrile (blue).

Influence of heteroatoms and geometry

The significant number of phosphonium salts synthesized possessing various five-membered heterocyclic rings provides the material for investigating the influence of heteroatoms on their photophysical properties. In-depth analysis however reveals that there is no clear correlation especially as far as fluorescence quantum yield is concerned. The comparison of salts **2d**, **2e** and **2f** based on benzothiophene, benzofuran and indole reveals almost no differences in emission intensity and only moderate bathochromic shift of emission for indole-based dye **2f**. Typically oxygen-to-sulfur swap leads to small HOMO destabilization.[61] However, in the case of **2d**,**e** the impact of the sulfur atom is barely distinguishable (Fig. 3, Table 1, Fig. S167 and S169†), suggesting that the PPh_2^+ moiety[62] strongly affects the electronic structure than the O to S displacement. There is however significant impact of geometry within for example phosphonium salts bearing indole scaffold (Table 1). Depending on the linkage position between indole moiety and quaternary phosphonium salt, the fluorescence quantum yield varies from almost quantitative to 2%. Interestingly the influence of heteroatom is visible for DHPPs **2j–2n**. Fluorescence quantum yield of benzothiophene-based dye **2j** is more than 20 times higher than for benzofuran-based **2k**, whereas the strongest fluorescence is in the case of salt **2l** possessing benzenes as flanking units. Again the change of geometry so that P-atom bridges positions 3 and 6 of DHPP core with *N*-phenyl (rather than *C*-phenyl) substituent causes large changes in photophysics including *e.g.* ≈60 nm hypsochromic shift of emission. The largest change however is caused by replacing quadrupolar centrosymmetric dyes **2j**, **2k**, **2l** with non-symmetrical salt **2m**. The latter one has weak but strongly bathochromically shifted emission (Table 1). On the

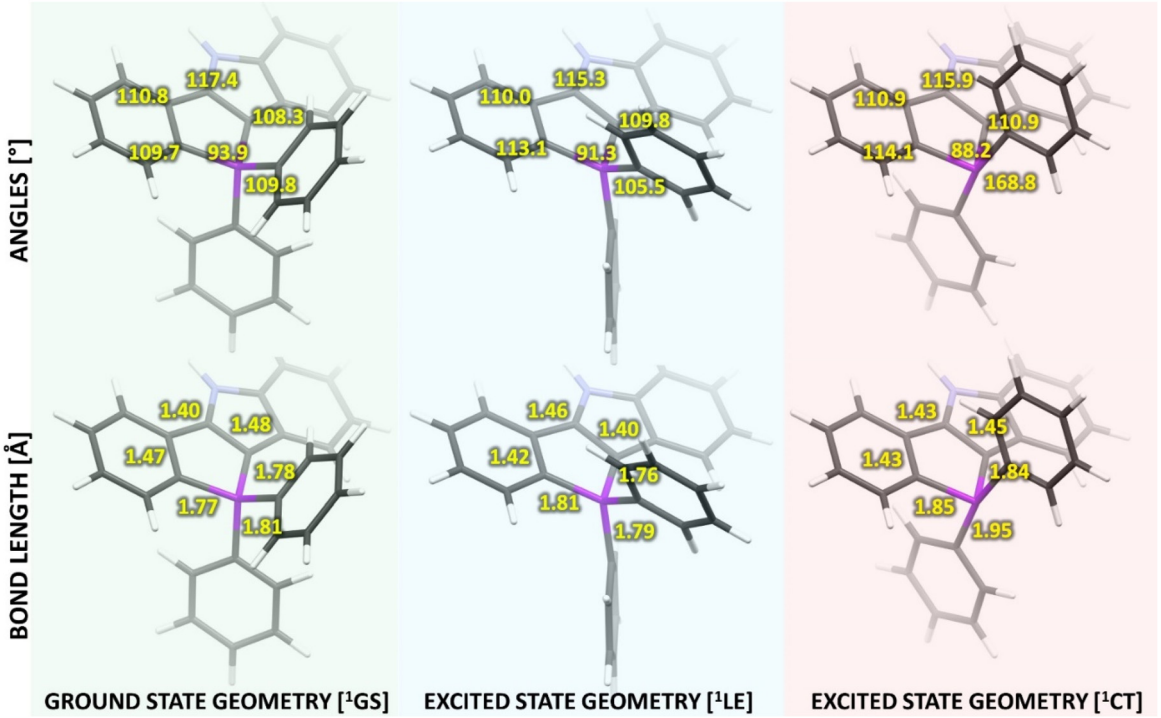

Fig. 2 Angles and bond lengths for **2f** in ground state (^{1}GS), local excited state (^{1}LE) and so-called charge transfer state (^{1}CT), visualizing the excitation-driven geometrical changes within the phospholium subunit.

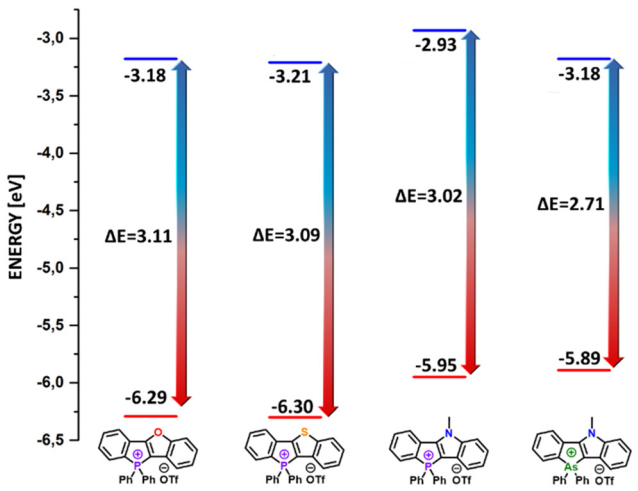

Fig. 3 Energy diagram representing changes in energy of frontier orbitals *vs.* the change of heteroatom. HOMO and LUMO levels are determined *via* cyclic voltammetry.

other hand, replacing P with As leads to a distinct stabilization of LUMO, indicating a stronger acceptor character of the arsolium compared to the phospholium subunit. Moreover, a heavier pnictogen atom distinctly affects fluorescence, making **6** a non-emissive salt. According to calculations, **6** after excitation to the ^{1}LE, which proves to be unstable, immediately rearranges to the ^{1}CT, located at the As$^+$ center (Fig. S242 and S245†). Then the intersection between ^{1}CT and ^{1}GS leads to intense internal conversion being responsible for the non-radiative deactivation of the excited state.

Impact of phosphacycle ring size

To investigate the influence of phosphacycle size on photophysics, salts **2g**,**h**,**i** were chosen due to their highest structural similarity. It has to be pointed out that the differences in substitution pattern (2-phenyl (**2g**) substitution *vs.* 4-phenyl substitution (**2h**)) slightly affect the electron density distribution within HOMO and its energy. Thus, observed changes can be correlated to phosphacycle size. Absorption spectra comparison indicates that the ring expansion, leads to a hypsochromic shift accompanied by the appearance of a distinct vibronic progression as well as a gradual rise of ε (Table 1, Fig. S174, S176 and S178†), from 371 nm (ε = 3800 M^{-1} cm^{-1}) for **2g** to 300 nm (ε = 15 800 M^{-1} cm^{-1}) for **2i** in dichloromethane.

These trends imply that upon phosphacycle expansion, distinct changes in electronic structure take place. While the energy of HOMO remains virtually unaffected, with the electron density distribution confined within the indole part (Tables S15, S16 and S18), the LUMO energy significantly rises passing from a five- to a seven-membered ring (Fig. 4) and causing blue-shift of the absorption spectrum. This results from a weaker impact of the P$^+$ center on orbital stabilization, due to a reduction of π^*–σ^* coupling contributions to LUMO (Tables S15, S16 and S18†). Moreover, ring expansion entails a significant drop in fluorescence quantum yield from ≈100%

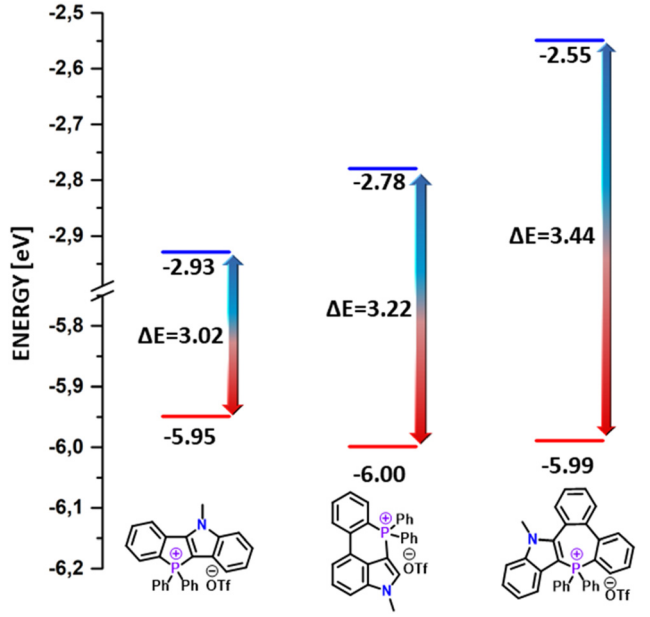

Fig. 4 Energy diagram representing changes in energy of frontier orbitals *vs.* ring size. HOMO and LUMO levels are determined *via* cyclic voltammetry.

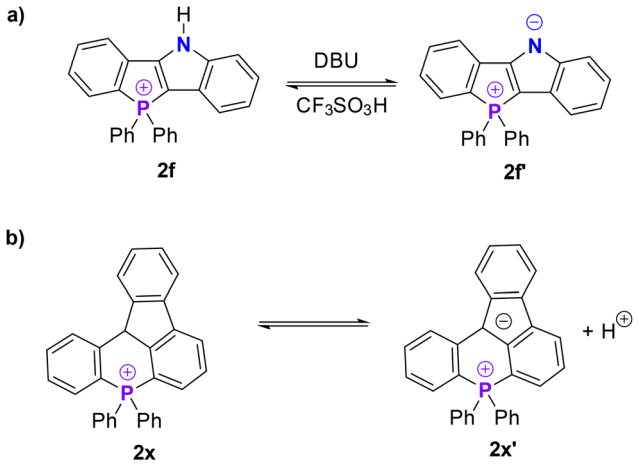

Scheme 4 Deprotonation of **2f** (a) and **2x** (b).

for **2g** to 2% for **2i**, as a result of intense deactivation of the excited state through the ^{1}CT nonradiative channel.

Photophysics of zwitterions

Among synthesized compounds, **2f** and **2x** possess an acidic hydrogen atom. Thus, in the presence of a base like 1,8-diazabicyclo(5.4.0)undec-7-ene (DBU), **2f,x** can be transformed into zwitterions. This process is notably reversible, meaning that upon TfOH addition, the uncharged species reverts to their cationic form. Interestingly, **2x** undergoes deprotonation even in the absence of a base, enabling estimation of its acidic dissociation constant (pK_a) in dichloromethane to be around 7.05 (eqn (S1)†). More than 10 orders of magnitude increase of the pK_a, compared to 9-phenylfluorene in dimethylsulfoxide (pK_a = 17.9),[63] reveals a strong influence of PPh_2^+ moiety on acidic properties enhancement. Moreover, the absorption spectra (Fig. S204†) of **2x** indicate a significant equilibrium shift (Scheme 4) to the right with increasing solvent polarity. As a result of the presence of two forms in the solution, double fluorescence can be observed in acetonitrile, with λ_{em} = 355 nm and 652 nm. Spectroscopic changes arising upon deprotonation are nicely illustrated in the case of **2f**, where a distinct absorption band at ≈355 nm (ε = 4500 M^{-1} cm^{-1}) becomes flattened (ε < 2500 M^{-1} cm^{-1}) after proton abstraction, thus determining λ_{abs} becomes challenging for **2f'** (Fig. S191†). The decrease of the molar extinction coefficient stands in line with the calculated oscillator strengths for the $S_0 \rightarrow S_1$ transition (for **2f**: f = 0.133 and **2f'**: f = 0.025). Passing from **2f** to the **2f'** also noticeably impacts the emissive properties, causing a bathochromic shift of the fluorescence spectrum of about 3000 cm^{-1} (Table 1, Fig. S171 and S173†), accompanied by a 26-times drop of Φ_{FL}. The ADC(2) method calculations performed for **2f** and **2f'** give deeper insight into the excited molecule deactivation process. According to the energy diagram (Fig. 5), deprotonation of **2f** significantly lowers the energy, not only of ^{1}LE, but also of the ^{1}CT state in **2f'**. Moreover, excited molecule relaxation causes the inversion of both the ^{1}LE and ^{1}CT states, leading to an intersection between ^{1}CT and ^{1}GS. Making ^{1}CT an intense nonradiative deactivation channel, resulting in residual fluorescence with Φ_{FL} ≈ 2% for **2f'**.

Fluorescence imaging

It is well-known that triarylphosphonium salts are anchors enabling the selective localization of fluorophores in mitochondria.[64–68] In 2019, the groups of Koshevoy, Romero-Nieto and Chou reported that a cyclic tetraarylphosphonium salt possessing an anthracene core also localizes in mitochondria.[24] Inspired by these observations,[28] we became curious whether our new cyclic tetraarylphosphonium salts could display analogous behavior. Salt **2g** was selected as a model system due to its strong green fluorescence (Table 1). We performed studies of the localization of dye **2g** in the U-87 cell line. The conducted fluorescence confocal microscopy experiments revealed that the subcellular distribution of salt **2g** produces a staining pattern consistent with selective mitochondrial localization after only a short incubation period (15–30 min) (Fig. 6A, Fig. S248–S250†). The selective intracellular localization of dye **2g** in U-87 cells was confirmed by co-localization with MitoTracker Red, a mitochondria-selective fluorescent label commonly used in confocal microscopy (Fig. 6B). The co-localization of salt **2g** with MitoTracker Red was confirmed by Fluorescence Resonance Energy Transfer (FRET) microscopy between the two compounds. Irradiation at 405 nm, the wavelength appropriate for salt **2g**, also excites the MitoTracker Red (Fig. 6A–C). The Pearson's coefficient (r = 0.676 ± 0.017) and Manders' coefficients (M1 = 0.894 ± 0.054

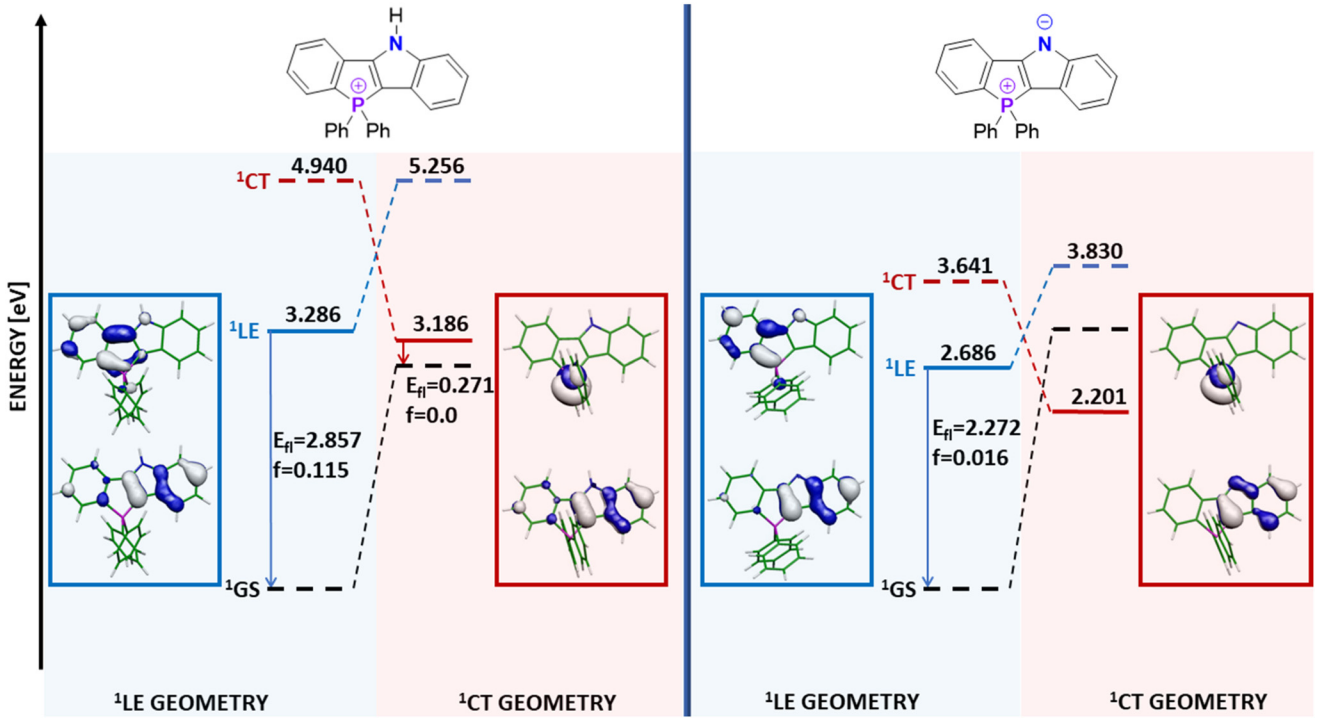

Fig. 5 A qualitative scheme of the excitation energies and radiative transitions of **2f** (left) and **2f*** (right) was obtained with the ADC(2) method. Solid lines denote the energies of the lowest excited singlet states (^{1}LE – blue and ^{1}CT – red) computed at their optimized equilibrium geometries. Dashed lines denote the respective state's energy calculated at the complementary state's equilibrium geometry. Vertical arrows represent fluorescence from the respective excited singlet state, with the energy of the vertical transition and the oscillator strength indicated. Molecular orbitals singly occupied in the relevant electronic state, LE-blue, and CT-red, are shown.

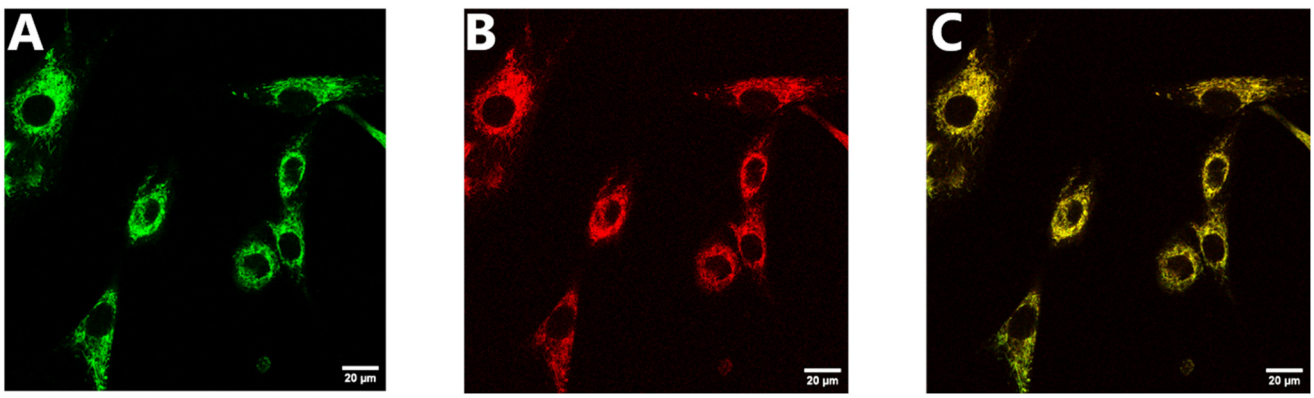

Fig. 6 Intracellular localization of **2g** compound and MitoTracker Red as detected using confocal fluorescence microscopy. (A) fluorescence of **2g** compound, excitation wavelength 405 nm, emission wavelength 500 ± 50 nm, (B) fluorescence of Mito Red compound, excitation wavelength 405 nm, emission wavelength 594 ± 50 nm. (C) overlay picture recorded sequentially as at (A) and (B) parameters for two fluorophores in living cells U-87. Scale bar 20 μm.

and M2 = 0.738 ± 0.091) of colocalization of salt **2g** and MitoTracker Red were calculated.

Conclusions

Phosphine oxides derived from heterocycles and polycyclic aromatic hydrocarbons can be activated with Tf_2O to form cyclic phosphonium salts integrated with the π-conjugated scaffold. Our strategy exhibits versatility concerning substrate scope, as both electron-rich and electron-neutral aromatics are compatible with this reaction. A broad range of π-conjugated phosphonium salts based on diverse aromatic scaffolds can be synthesized easily, in good yield, and without chromatographic purification. The method's versatility has been showcased by

incorporating such demanding moieties as azulene, 1,4-dihydropyrrolo[3,2-*b*]pyrrole and 5-oxatruxene. Importantly, arsonium salts could also be assessed, suggesting that this route could be easily adapted for the preparation of further derivatives. Critically, the photophysical properties of quaternary salts are affected by the type of fused heterocycle, the size of the phosphacycle, and π-expansion. Our strategy allowed rapid access to new cationic dyes, which often possessed both strong fluorescence as well as an emission wavelength strongly dependent on the phosphacycle size. *Ab initio* calculations revealed that competition between ^{1}LE and ^{1}CT is the key factor influencing the photophysical characteristics and determines the fate of the molecule's excited state. This discovery will provide the impetus for future explorations that use cyclic tetraarylphosphonium salts.

Author contributions

K.G. conceived the idea. K.G. and Ł.W.C. performed all synthetic experiments. A.W. performed imaging studies and A.S. supervised them. A.L.S. performed computational studies, analyzed data, wrote and reviewed the manuscript. D.T.G. supervised the project, performed formal analysis, and wrote and reviewed the manuscript. All the authors discussed the results and commented on the manuscript. All authors have approved the final version of the manuscript.

Data availability

The data supporting the article has been included as part of the ESI.†

Conflicts of interest

There are no conflicts to declare.

Acknowledgements

This project has received funding from the European Union's Horizon 2020 Research and Innovation Program under the Marie Skłodowska-Curie grant agreement no. 101007804 and from European Research Council (ARCHIMEDES, 101097337). Views and opinions expressed are, however, those of the authors only and do not necessarily reflect those of the European Union or the European Research Council Executive Agency. Neither the European Union nor the granting authority can be held responsible for them. The work was also financially supported by the Polish National Science Centre, Poland (OPUS 2020/37/B/ST4/00017). We thank Joseph Milton and Natalia D. Gryko for English proofreading.

References

1 A. Borissov, Y. K. Maurya, L. Moshniaha, W.-S. Wong, M. Żyła-Karwowska and M. Stępień, Recent Advances in Heterocyclic Nanographenes and Other Polycyclic Heteroaromatic Compounds, *Chem. Rev.*, 2022, **122**, 565–788.
2 M. Stępień, E. Gońka, M. Żyła and N. Sprutta, Heterocyclic Nanographenes and Other Polycyclic Heteroaromatic Compounds: Synthetic Routes, Properties, and Applications, *Chem. Rev.*, 2017, **117**, 3479–3716.
3 T. Baumgartner, Insights on the Design and Electron-Acceptor Properties of Conjugated Organophosphorus Materials, *Acc. Chem. Res.*, 2014, **47**, 1613–1622.
4 M. Stolar and T. Baumgartner, Phosphorus–Containing Materials for Organic Electronics, *Chem. – Asian J.*, 2014, **9**, 1212–1225.
5 E. Regulska, P. Hindenberg, A. Espineira-Gutierrez and C. Romero-Nieto, Synthesis, Post–Functionalization and Properties of Diphosphapentaarenes, *Chem. – Eur. J.*, 2023, **29**, e202202769.
6 N. König, Y. Godínez-Loyola, H. Weiske, S. Naumov, P. Lönnecke, R. Tonner-Zech, C. A. Strassert and E. Hey-Hawkins, Access to Strong Thieno[3,2-b]phosphole-Based Solid-State Emitters via Manganese(III)-Mediated Oxidative Annulation, *Chem. Mater.*, 2023, **35**, 8218–8228.
7 J. Fidelius, K. Schwedtmann, S. Schellhammer, J. Haberstroh, S. Schulz, R. Huang, M. C. Klotzsche, A. Bauzá, A. Frontera, S. Reineke and J. J. Weigand, Convenient access to π-conjugated 1,3-azaphospholes from alkynes via [3 + 2]-cycloaddition and reductive aromatization, *Chem*, 2024, **10**, 644–659.
8 K. Nishimura, K. Hirano and M. Miura, Direct Synthesis of Dibenzophospholes from Biaryls by Double C–P Bond Formation via Phosphenium Dication Equivalents, *Org. Lett.*, 2020, **22**, 3185–3189.
9 P. Hibner-Kulicka, J. A. Joule, J. Skalik and P. Bałczewski, Recent studies of the synthesis, functionalization, optoelectronic properties and applications of dibenzophospholes, *RSC Adv.*, 2017, **7**, 9194–9236.
10 H. Hattori, K. Ishida and N. Sakai, Synthetic Strategies for Accessing Dibenzophosphole Scaffolds, *Synthesis*, 2024, 193–219.
11 M. P. Duffy, W. Delaunay, P.-A. Bouit and M. Hissler, π-Conjugated phospholes and their incorporation into devices: components with a great deal of potential, *Chem. Soc. Rev.*, 2016, **45**, 5296–5310.
12 Z. Wang, B. S. Gelfand and T. Baumgartner, Dithienophosphole–Based Phosphinamides with Intriguing Self–Assembly Behavior, *Angew. Chem., Int. Ed.*, 2016, **55**, 3481–3485.
13 S. Nieto, P. Metola, V. M. Lynch and E. V. Anslyn, Synthesis of a Novel Bisphosphonium Salt Based on 2,2′-Bis(diphenylphosphino)-1,1′-binaphthyl (Binap), *Organometallics*, 2008, **27**, 3608–3610.
14 A. Fukazawa, E. Yamaguchi, E. Ito, H. Yamada, J. Wang, S. Irle and S. Yamaguchi, Zwitterionic Ladder Stilbenes

with Phosphonium and Borate Bridges: Intramolecular Cascade Cyclization and Structure–Photophysical Properties Relationship, *Organometallics*, 2011, **30**, 3870–3879.

15 L. Qiu, W. Hu, D. Wu, Z. Duan and F. Mathey, Regioselective Synthesis of 2- or 2,7-Functionalized Pyrenes via Migration, *Org. Lett.*, 2018, **20**, 7821–7824.

16 X. Zhao, Z. Gan, C. Hu, Z. Duan and F. Mathey, Planar Polycyclic Oxaphosphoranes Incorporating a Benzophosphole Unit, *Org. Lett.*, 2017, **19**, 5814–5817.

17 P.-A. Bouit, A. Escande, R. Szűcs, D. Szieberth, C. Lescop, L. Nyulászi, M. Hissler and R. Réau, Dibenzophosphapentaphenes: Exploiting P Chemistry for Gap Fine-Tuning and Coordination-Driven Assembly of Planar Polycyclic Aromatic Hydrocarbons, *J. Am. Chem. Soc.*, 2012, **134**, 6524–6527.

18 Y. Ren, W. H. Kan, M. A. Henderson, P. G. Bomben, C. P. Berlinguette, V. Thangadurai and T. Baumgartner, External-Stimuli Responsive Photophysics and Liquid Crystal Properties of Self-Assembled "Phosphole-Lipids", *J. Am. Chem. Soc.*, 2011, **133**, 17014–17026.

19 Y. Koyanagi, S. Kawaguchi, K. Fujii, Y. Kimura, T. Sasamori, N. Tokitoh and Y. Matano, Effects of counter anions, P-substituents, and solvents on optical and photophysical properties of 2-phenylbenzo[b]phospholium salts, *Dalton Trans.*, 2017, **46**, 9517–9527.

20 T. Delouche, A. Vacher, E. Caytan, T. Roisnel, B. Le Guennic, D. Jacquemin, M. Hissler and P. Bouit, Multi–Stage Redox Systems Based on Dicationic P–Containing Polycyclic Aromatic Hydrocarbons, *Chem. – Eur. J.*, 2020, **26**, 8226–8229.

21 P. Hindenberg, F. Rominger and C. Romero-Nieto, Phosphorus Post–Functionalization of Diphosphahexaarenes, *Chem. – Eur. J.*, 2019, **25**, 13146–13151.

22 P. Hindenberg, A. López-Andarias, F. Rominger, A. de Cózar and C. Romero-Nieto, A Guide for the Design of Functional Polyaromatic Organophosphorus Materials, *Chem. – Eur. J.*, 2017, **23**, 13919–13928.

23 T. A. Schaub, S. M. Brülls, P. O. Dral, F. Hampel, H. Maid and M. Kivala, Organic Electron Acceptors Comprising a Dicyanomethylene–Bridged Acridophosphine Scaffold: The Impact of the Heteroatom, *Chem. – Eur. J.*, 2017, **23**, 6988–6992.

24 A. Belyaev, Y. Chen, Z. Liu, P. Hindenberg, C. Wu, P. Chou, C. Romero-Nieto and I. O. Koshevoy, Intramolecular Phosphacyclization: Polyaromatic Phosphonium P–Heterocycles with Wide–Tuning Optical Properties, *Chem. – Eur. J.*, 2019, **25**, 6332–6341.

25 S. Arndt, M. M. Hansmann, F. Rominger, M. Rudolph and A. S. K. Hashmi, Direct Access to π–Extended Phosphindolium Salts by Simple Proton–Induced Cyclization of (o –Alkynylphenyl)phosphanes, *Chem. – Eur. J.*, 2017, **23**, 5429–5433.

26 B. Yang, S. Yan, C. Li, H. Ma, F. Feng, Y. Zhang and W. Huang, Mn(iii)-mediated C–P bond activation of diphosphines: toward a highly emissive phosphahelicene cation scaffold and modulated circularly polarized luminescence, *Chem. Sci.*, 2023, **14**, 10446–10457.

27 A. Belyaev, Y.-T. Chen, S.-H. Su, Y.-J. Tseng, A. J. Karttunen, S. P. Tunik, P.-T. Chou and I. O. Koshevoy, Copper-mediated phospha-annulation to attain water-soluble polycyclic luminophores, *Chem. Commun.*, 2017, **53**, 10954–10957.

28 K. Andoh, M. Murai, P. Bouit, M. Hissler and S. Yamaguchi, Dithieno[3,2– b; 2′,3′– f]phosphepinium–Based Near–Infrared Fluorophores: p x –π* Conjugation Inherent to Seven–Membered Phosphacycles, *Angew. Chem., Int. Ed.*, 2024, **63**, e202410204.

29 A. Fukazawa, H. Yamada and S. Yamaguchi, Phosphonium– and Borate–Bridged Zwitterionic Ladder Stilbene and Its Extended Analogues, *Angew. Chem., Int. Ed.*, 2008, **47**, 5582–5585.

30 X. He, J. Lin, W. H. Kan and T. Baumgartner, Phosphinine Lipids: A Successful Marriage between Electron–Acceptor and Self–Assembly Features, *Angew. Chem., Int. Ed.*, 2013, **52**, 8990–8994.

31 J. C. Chan, W. H. Lam, H. Wong, W. Wong and V. W. Yam, Tunable Photochromism in Air–Stable, Robust Dithienylethene–Containing Phospholes through Modifications at the Phosphorus Center, *Angew. Chem., Int. Ed.*, 2013, **52**, 11504–11508.

32 E. Yamaguchi, C. Wang, A. Fukazawa, M. Taki, Y. Sato, T. Sasaki, M. Ueda, N. Sasaki, T. Higashiyama and S. Yamaguchi, Environment–Sensitive Fluorescent Probe: A Benzophosphole Oxide with an Electron–Donating Substituent, *Angew. Chem., Int. Ed.*, 2015, **54**, 4539–4543.

33 Y. Ren, W. H. Kan, V. Thangadurai and T. Baumgartner, Bio–Inspired Phosphole–Lipids: From Highly Fluorescent Organogels to Mechanically Responsive FRET, *Angew. Chem., Int. Ed.*, 2012, **51**, 3964–3968.

34 (*a*) Y. Matano, A. Saito, T. Fukushima, Y. Tokudome, F. Suzuki, D. Sakamaki, H. Kaji, A. Ito, K. Tanaka and H. Imahori, Fusion of Phosphole and 1,1′–Biacenaphthene: Phosphorus(v)–Containing Extended π–Systems with High Electron Affinity and Electron Mobility, *Angew. Chem.*, 2011, **123**, 8166–8170; (*b*) P. Federmann, H. K. Wagner, P. W. Antoni, J.-M. Mörsdorf, J. L. Pérez Lustres, H. Wadepohl, M. Motzkus and J. Ballmann, A 2,2′-diphosphinotolane as a versatile precursor for the synthesis of P-ylidic mesoionic carbenes *via* reversible C–P bond formation, *Org. Lett.*, 2019, **21**, 2033–2038.

35 Y. Wang, G. Su, M. Li, L. Yao, W. A. Chalifoux and W. Yang, Synthesis of P-Containing Polycyclic Aromatic Hydrocarbons from Alkynyl-phosphonium Salts, *Org. Lett.*, 2024, **26**, 5280–5284.

36 K. Yasuda and S. Ito, A π–Extension Process from 9–Phosphaanthracene Leading to Phosphatetraphenes and Phosphatetracenes, *ChemPlusChem*, 2023, **88**, e202300277.

37 P. de Koe and F. Bickelhaupt, 10–Phenyldibenzo[b,e]phosphorin, *Angew. Chem., Int. Ed. Engl.*, 1968, **7**, 889–890.

38 T. Baumgartner and R. Réau, Organophosphorus π-Conjugated Materials (Chem. Rev. 2006, 106, 4681–4727.

Published on the Web November 8, 2006.), *Chem. Rev.*, 2007, **107**, 303–303.

39 J. W. Heinicke, Electron–Rich Aromatic 1,3–Heterophospholes – Recent Syntheses and Impact of High Electron Density at σ 2 P on the Reactivity, *Eur. J. Inorg. Chem.*, 2016, **2016**, 575–594.

40 S. Wu, A. L. Rheingold, J. A. Golen, A. B. Grimm and J. D. Protasiewicz, Synthesis of a Luminescent Azaphosphole, *Eur. J. Inorg. Chem.*, 2016, **2016**, 768–773.

41 J. P. Bard, S. G. Bolton, H. J. Howard, J. N. McNeill, T. P. de Faria, L. N. Zakharov, D. W. Johnson, M. D. Pluth and M. M. Haley, 2-λ 5 -Phosphaquinolin-2-ones as Non-cytotoxic, Targetable, and pH-Stable Fluorophores, *J. Org. Chem.*, 2023, **88**, 15516–15522.

42 J. P. Bard, H. J. Bates, C.-L. Deng, L. N. Zakharov, D. W. Johnson and M. M. Haley, Amplification of the Quantum Yields of 2-λ 5 -Phosphaquinolin-2-ones through Phosphorus Center Modification, *J. Org. Chem.*, 2020, **85**, 85–91.

43 S. Arndt, M. M. Hansmann, P. Motloch, M. Rudolph, F. Rominger and A. S. K. Hashmi, Intramolecular anti –Phosphinoauration of Alkynes: An FLP–Motivated Approach to Stable Aurated Phosphindolium Complexes, *Chem. – Eur. J.*, 2017, **23**, 2542–2547.

44 T. Zhang, M. Cai, W. Zhao, M. Liu, N. Jiang, Q. Ge and H. Cong, Electrochemical oxidative intramolecular annulation of aryl phosphine compounds: an efficient approach for synthesizing π-conjugated phosphonium salts, *Green Chem.*, 2023, **25**, 1351–1355.

45 S. Ishikawa and K. Manabe, Synthesis of hydroxylated oligoarene-type phosphines by a repetitive two-step method, *Tetrahedron*, 2010, **66**, 297–303.

46 K. Nishimura, K. Hirano and M. Miura, Synthesis of Dibenzophospholes by Tf 2 O-Mediated Intramolecular Phospha-Friedel–Crafts-Type Reaction, *Org. Lett.*, 2019, **21**, 1467–1470.

47 Y. Unoh, K. Hirano and M. Miura, Metal-Free Electrophilic Phosphination/Cyclization of Alkynes, *J. Am. Chem. Soc.*, 2017, **139**, 6106–6109.

48 K. Nishimura, Y. Unoh, K. Hirano and M. Miura, Phosphenium–Cation–Mediated Formal Cycloaddition Approach to Benzophospholes, *Chem. – Eur. J.*, 2018, **24**, 13089–13092.

49 A. Janiga, E. Glodkowska-Mrowka, T. Stoklosa and D. T. Gryko, Synthesis and Optical Properties of Tetraaryl–1,4–dihydropyrrolo[3,2–b]pyrroles, *Asian J. Org. Chem.*, 2013, **2**, 411–415.

50 M. Krzeszewski, Ł. Dobrzycki, A. L. Sobolewski, M. K. Cyrański and D. T. Gryko, Saddle-shaped aza-nanographene with multiple odd-membered rings, *Chem. Sci.*, 2023, **14**, 2353–2360.

51 T. V. RajanBabu, N. S. Simpkins and T. V. RajanBabu, in *Encyclopedia of Reagents for Organic Synthesis*, John Wiley & Sons, Ltd, Chichester, UK, 2005.

52 V. Brega, S. N. Kanari, C. T. Doherty, D. Che, S. A. Sharber and S. W. Thomas, Spectroscopy and Reactivity of Dialkoxy Acenes, *Chem. – Eur. J.*, 2019, **25**, 10400–10407.

53 K. Górski, J. Mech-Piskorz and M. Pietraszkiewicz, From truxenes to heterotruxenes: playing with heteroatoms and the symmetry of molecules, *New J. Chem.*, 2022, **46**, 8939–8966.

54 K. Górski, D. Kusy, S. Ozaki, M. Banasiewicz, R. Valiev, S. R. Sahoo, K. Kamada, G. Baryshnikov and D. T. Gryko, The interplay of intersystem crossing and internal conversion in quadrupolar tetraarylpyrrolo[3,2-b]pyrroles, *J. Mater. Chem. C*, 2024, **12**, 1980–1987.

55 T. Ma, J. Dong and D.-T. Yang, Heteroatom-boron-heteroatom-doped π-conjugated systems: structures, synthesis and photofunctional properties, *Chem. Commun.*, 2023, **59**, 13679–13689.

56 H. A. Frank, J. A. Bautista, J. Josue, Z. Pendon, R. G. Hiller, F. P. Sharples, D. Gosztola and M. R. Wasielewski, Effect of the Solvent Environment on the Spectroscopic Properties and Dynamics of the Lowest Excited States of Carotenoids, *J. Phys. Chem. B*, 2000, **104**, 4569–4577.

57 A. Marini, A. Muñoz-Losa, A. Biancardi and B. Mennucci, What is Solvatochromism?, *J. Phys. Chem. B*, 2010, **114**, 17128–17135.

58 K. Górski, I. Deperasińska, G. V. Baryshnikov, S. Ozaki, K. Kamada, H. Ågren and D. T. Gryko, Quadrupolar Dyes Based on Highly Polarized Coumarins, *Org. Lett.*, 2021, **23**, 6770–6774.

59 J. P. Cerón-Carrasco, D. Jacquemin, C. Laurence, A. Planchat, C. Reichardt and K. Sraïdi, Solvent polarity scales: determination of new E T (30) values for 84 organic solvents, *J. Phys. Org. Chem.*, 2014, **27**, 512–518.

60 J. Catalán, Toward a Generalized Treatment of the Solvent Effect Based on Four Empirical Scales: Dipolarity (SdP, a New Scale), Polarizability (SP), Acidity (SA), and Basicity (SB) of the Medium, *J. Phys. Chem. B*, 2009, **113**, 5951–5960.

61 K. Górski, K. Noworyta and J. Mech-Piskorz, Influence of the heteroatom introduction on the physicochemical properties of 5-heterotruxenes containing nitrogen, oxygen and sulfur atom, *RSC Adv.*, 2020, **10**, 42363–42377.

62 C. Fave, M. Hissler, T. Kárpáti, J. Rault-Berthelot, V. Deborde, L. Toupet, L. Nyulászi and R. Réau, Connecting π-Chromophores by σ-P–P Bonds: New Type of Assemblies Exhibiting σ–π-Conjugation, *J. Am. Chem. Soc.*, 2004, **126**, 6058–6063.

63 W. S. Matthews, J. E. Bares, J. E. Bartmess, F. G. Bordwell, F. J. Cornforth, G. E. Drucker, Z. Margolin, R. J. McCallum, G. J. McCollum and N. R. Vanier, Equilibrium acidities of carbon acids. VI. Establishment of an absolute scale of acidities in dimethyl sulfoxide solution, *J. Am. Chem. Soc.*, 1975, **97**, 7006–7014.

64 Q. Hu, M. Gao, G. Feng and B. Liu, Mitochondria–Targeted Cancer Therapy Using a Light–Up Probe with Aggregation–Induced–Emission Characteristics, *Angew. Chem., Int. Ed.*, 2014, **53**, 14225–14229.

65 C. W. T. Leung, Y. Hong, S. Chen, E. Zhao, J. W. Y. Lam and B. Z. Tang, A Photostable AIE Luminogen for Specific Mitochondrial Imaging and Tracking, *J. Am. Chem. Soc.*, 2013, **135**, 62–65.

66 R. Roopa, N. Kumar, V. Bhalla and M. Kumar, Development and sensing applications of fluorescent motifs within the mitochondrial environment, *Chem. Commun.*, 2015, **51**, 15614–15628.
67 H. Ogasawara, Y. Tanaka, M. Taki and S. Yamaguchi, Late-stage functionalisation of alkyne-modified phospha-xanthene dyes: lysosomal imaging using an off–on–off type of pH probe, *Chem. Sci.*, 2021, **12**, 7902–7907.
68 G. D. Kumar, M. Banasiewicz, A. Wrzosek, R. P. Kampa, M. H. E. Bousquet, D. Kusy, D. Jacquemin, A. Szewczyk and D. T. Gryko, Probing the flux of mitochondrial potassium using an azacrown-diketopyrrolopyrrole based highly sensitive probe, *Chem. Commun.*, 2022, **58**, 4500–4503.